

Dynamical theory of single-photon transport through a qubit chain coupled to a one-dimensional nanophotonic waveguide

Ya. S. Greenberg,* O. A. Chuikin, A. A. Shtygashev, and A. G. Moiseev
Novosibirsk State Technical University, Novosibirsk, Russia

(Dated: February 8, 2024)

We study the dynamics of a single-photon pulse travelling through a linear qubit chain coupled to continuum modes in a one-dimensional (1D) photonic waveguide. We derive a time-dependent dynamical theory for qubit amplitudes and for transmitted and reflected spectra. We show that the requirement for the photon-qubit coupling to exist only for positive frequencies can significantly change the dynamics of the system. First, it leads to an additional photon-mediated dipole-dipole interaction between qubits which results in the violation of the phase coherence between them. Second, the spectral lines of transmitted and reflected spectra crucially depend on the shape of the incident pulse and the initial distance between the pulse center and the first qubit in the chain. We apply our theory to one-qubit and two-qubit systems. For these two cases, we obtain the explicit expressions for the qubits' amplitudes and for the photon radiation spectra as time tends to infinity. For the incident Gaussian wave packet we calculate the line shapes of transmitted and reflected photons.

I. INTRODUCTION

Manipulating the propagation of photons in a one-dimensional waveguide coupled to an array of two-level atoms (qubits) may have important applications in quantum devices and quantum information technologies [1–4].

Quantum bits can be implemented with a variety of quantum systems, such as trapped ions [5], photons [6–8], and quantum dots [9, 10]. In particular, superconducting qubits [11, 12] have emerged as one of the leading candidate for scalable quantum processor architecture.

Transmission of a single photon through an array of two-level atoms embedded in a 1D open waveguide has been extensively studied both theoretically [13–15] and experimentally [16–18].

Most theoretical calculations of the transmitted and reflected photon amplitudes in a 1D open waveguide with atoms placed inside have been performed within the framework of the stationary theory in a configuration space [19–22] or by alternative methods such as those based on Lippmann-Schwinger scattering theory [23–25], input-output formalism [14, 26, 27], non-Hermitian Hamiltonian [28], and matrix methods [29, 30].

Even though the stationary theory of the photon transport provides a useful guide to what one would expect in real experiment, it does not allow for a description of the dynamics of a qubit excitation and the evolution of the scattered photon amplitudes.

In practice, qubits are excited by photon pulses of finite duration and finite bandwidth. Therefore, to study the real-time evolution of photon transport and atomic excitation the time-dependent dynamical theory has been developed [31–35]. This theory relies on two assumptions. The first is the Wigner-Weisskopf approximation in which the rate of spontaneous emission to the

guided mode is much less than the qubit frequency, $\Gamma(\omega) \ll \Omega$. Therefore, the decay rate Γ is assumed frequency-independent and is considered at the resonant frequency Ω , $\Gamma(\omega) = \Gamma(\Omega) \equiv \Gamma$. The second assumption is more subtle. It is assumed that the photon-mediated coupling $g(\omega)$ may be extended to negative frequencies which allows to move the lower bound of some frequency integrals to minus infinity. In this case, the transmitted and reflected photon amplitudes become proportional to the spectral density of incident pulse, $\gamma_0(\omega)$ [32]. It is believed that the continuation of $g(\omega)$ to negative frequencies is justified beyond rotating wave approximation (RWA) by accounting for counter rotating terms (see Supplement in [36]). The extension to negative frequencies are generally relies on the assumption that non-RWA contribution is negligible which is not always the case. Moreover, it is not justified from physical arguments: because the continuum starts at $\omega = 0$, the density of states is zero for $\omega < 0$. Therefore, $g(\omega) = 0$ for $\omega < 0$, that is the coupling does not exist at negative frequencies [37]. Thus, its continuation to negative frequencies makes no sense. From the other hand, we may consider this continuation as a pure mathematical trick which can be justified if the negative frequency integral provides a small correction. This is indeed the case if the distance between qubits d exceeds the qubit wavelength $\lambda = 2\pi v_g/\Omega$. However, if $d < \lambda$ the discrepancy can be significant (see Appendix B in [38]).

Another consequence of "no continuation" of $g(\omega)$ to negative frequencies is more complicated dependence of photon radiation on the shape of incident pulse: the transmitted and reflected photon amplitudes are no longer proportional to $\gamma_0(\omega)$.

From the point of view of device applications, a control pulse generator should be placed as close as possible to the measured qubit circuitry, for example, in the same chip with superconducting qubit at millikelvin temperatures [39]. We show that such an arrangement leads to significant modifications of the photon radiation spectra

*Electronic address: yakovgreenberg@yahoo.com

if the distance between the initial position of the peak of an incident pulse and the first qubit in a chain is comparable to or less than the pulse width in configuration space.

The paper is organized as follows. In Section II we briefly describe our system consisting of N identical qubits in a one-dimensional infinite waveguide. The system is described by Jaynes-Cummings Hamiltonian in rotating wave approximation (RWA). The Hilbert space is restricted to the single-excitation subspace.

In Section III the general time-dependent equations for qubits' amplitudes, $\beta_n(t)$ and photon forward, $\gamma(\omega, t)$ and backward $\delta(\omega, t)$ radiation spectra for a single-photon pulse scattering from an array of N identical qubits are derived. These equations are then solved by application of Heitler's method, which allows us to find the desired solutions for time-dependent amplitudes. The main result of this section is the modification of the equations for qubits amplitudes which appears due to non continuation of the interqubit interaction to negative frequencies (see Eq.25). First, it leads to the additional photon-mediated dipole-dipole interaction between qubits which results in the violation of the phase coherence between them. Second, the spectral lines of transmitted and reflected spectra crucially depend on the shape of incident pulse and on the initial distance between the pulse center and first qubit in the chain.

The theoretical results obtained in Section III are applied for the calculations of photon forward and backward radiation spectra for scattering of a moving Gaussian pulse from a single qubit (Section IV) and from two-qubit system (Section V). We show that the form of radiation spectra crucially depends on the distance between the initial position of Gaussian peak and the first qubit in a chain. The radiation spectra are substantially modified if this distance is comparable to or less than the pulse width in a configuration space.

Summary of our work is presented in the conclusion (Section VI). Some additional technical calculations are given in Appendixes.

II. THE MODEL

We consider a system consisting of N identical qubits in a one-dimensional infinite waveguide. In the continuum mode representation this system can be described by a Jaynes-Cummings Hamiltonian which accounts for the interaction between qubits and electromagnetic field [40, 41] (from now on we use the units $\hbar = 1$ throughout the paper, therefore, all energies are expressed in frequency

units):

$$\begin{aligned}
 H = & \frac{1}{2} \sum_{n=1}^N \left(1 + \sigma_z^{(n)}\right) \Omega \\
 & + \int_0^\infty \omega a^\dagger(\omega) a(\omega) d\omega + \int_0^\infty \omega b^\dagger(\omega) b(\omega) d\omega \\
 & + \int_0^\infty a^\dagger(\omega) S_-(\omega) d\omega + \int_0^\infty a(\omega) S_+(\omega) d\omega \\
 & + \int_0^\infty b^\dagger(\omega) S_-^*(\omega) d\omega + \int_0^\infty b(\omega) S_+^*(\omega) d\omega,
 \end{aligned} \tag{1}$$

where $\sigma_z^{(n)}$ is a Pauli spin operator, Ω is a resonant frequency of n th qubit, ω is a photon frequency.

The photon creation and annihilation operators $a^\dagger(\omega)$, $a(\omega)$, and $b^\dagger(\omega)$, $b(\omega)$ describe forward and backward scattering waves, respectively. They are independent of each other and satisfy the usual continuous-mode commutation relations [40]:

$$[a(\omega), a^\dagger(\omega')] = [b(\omega), b^\dagger(\omega')] = \delta(\omega - \omega'). \tag{2}$$

In (1) we introduced collective atomic spin operators:

$$\begin{aligned}
 S_-(\omega) &= \sum_{n=1}^N g(\omega) e^{-ikx_n} \sigma_-^{(n)}, \\
 S_+(\omega) &= \sum_{n=1}^N g(\omega) e^{ikx_n} \sigma_+^{(n)}.
 \end{aligned} \tag{3}$$

where $k = \omega/v_g$, v_g is the group velocity of electromagnetic waves, x_n is a spatial coordinate of the n th qubit. $\sigma_-^{(n)} = |g\rangle_{nn} \langle e|$ and $\sigma_+^{(n)} = |e\rangle_{nn} \langle g|$ are the lowering and raising atomic operators which lower or raise a state of the n th qubit. A spin operator $\sigma_z^{(n)} = |e\rangle_{nn} \langle e| - |g\rangle_{nn} \langle g|$. The quantity $g(\omega)$ in (1) is the coupling between qubit and the photon field in a waveguide [41]:

$$g(\omega) = \sqrt{\frac{\omega d^2}{4\pi\epsilon_0 \hbar v_g S}}, \tag{4}$$

where d is the off diagonal matrix element of a dipole operator, S is the effective transverse cross section of the modes in one-dimensional waveguide, v_g is the group velocity of electromagnetic waves. We assume that the coupling is the same for forward and backward waves.

Note that the dimension of the coupling constant $g(\omega)$ is not a frequency, ω but a square of frequency, $\sqrt{\omega}$, and, as it follows from (2), the dimension of creation and annihilation operators is $1/\sqrt{\omega}$.

Below we consider a single-excitation subspace with either a single photon is in a waveguide and all qubits are in the ground state, or there are no photons in a waveguide with the only n th qubit in the chain being

excited. Therefore, we truncate Hilbert space to the following states:

$$\begin{aligned} |G, 1_k\rangle &= |g_1, g_2, \dots, g_N\rangle \otimes |1_k\rangle; \\ |n, 0_k\rangle &= |g_1, g_2, \dots, g_{n-1}, e_n, g_{n+1}, \dots, g_N\rangle \otimes |0_k\rangle; \end{aligned} \quad (5)$$

The Hamiltonian (1) preserves the number of excitations (number of excited qubits + number of photons). In our case the number of excitations is equal to one. Therefore, at any instant of time the system will remain within a single-excitation subspace.

The trial wave function of an arbitrary single-excitation state can then be written in the form:

$$\begin{aligned} \Psi(t) &= \sum_{n=1}^N \beta_n(t) e^{-i\Omega t} |n, 0\rangle \\ &+ \int_0^\infty d\omega \gamma(\omega, t) e^{-i\omega t} a^\dagger(\omega) |G, 0\rangle \\ &+ \int_0^\infty d\omega \delta(\omega, t) e^{-i\omega t} b^\dagger(\omega) |G, 0\rangle, \end{aligned} \quad (6)$$

where $\beta_n(t)$ is the amplitude of n th qubit, $\gamma(\omega, t)$ and $\delta(\omega, t)$ are single-photon amplitudes which are related to a spectral density of forward and backward radiation, respectively.

III. EQUATIONS FOR QUBITS' AND PHOTON AMPLITUDES

The Schrodinger equation $i \frac{d\Psi(t)}{dt} = H\Psi(t)$ yields the equations for the amplitudes:

$$\begin{aligned} \frac{d\beta_n}{dt} &= -i \int_0^\infty d\omega g(\omega) \gamma(\omega, t) e^{ikx_n} e^{-i(\omega-\Omega)t} \\ &- i \int_0^\infty d\omega g(\omega) \delta(\omega, t) e^{-ikx_n} e^{-i(\omega-\Omega)t}, \end{aligned} \quad (7)$$

$$\frac{d\gamma(\omega, t)}{dt} = -ig(\omega) e^{i(\omega-\Omega)t} \sum_{n=1}^N \beta_n(t) e^{-ikx_n}, \quad (8)$$

$$\frac{d\delta(\omega, t)}{dt} = -ig(\omega) e^{i(\omega-\Omega)t} \sum_{n=1}^N \beta_n(t) e^{ikx_n}. \quad (9)$$

The system equations (7), (8), and (9) have a physical sense only for $t > 0$. Therefore they should be supplemented by the initial conditions:

$$\beta_n(0) = 0; \delta(\omega, 0) = 0; \gamma(\omega, +0) = \gamma_0(\omega) \quad (10)$$

where $\gamma_0(\omega)$ is the initial incident pulse which for a single scattering photon is assumed to be normalized to unity, $\int_0^\infty d\omega |\gamma_0(\omega)|^2 = 1$.

For the analytical reasons it is convenient to extend, by the Heitler method [42], the solution of system (7), (8), and (9) to the negative time semi axis, assuming that

$$\beta_n(t) = 0; \delta(\omega, t) = 0; \gamma(\omega, t) = 0; t < 0 \quad (11)$$

Therefore, the amplitudes $\beta_n(t)$ and $\delta(\omega, t)$ are continuous over the entire time axis, while the function $\gamma(\omega, t)$ has a jump at $t = 0$. We will take this into account by adding the inhomogeneous term into the equation (8):

$$\frac{d\gamma(\omega, t)}{dt} = -ig(\omega) e^{i(\omega-\Omega)t} \sum_{n=1}^N \beta_n(t) e^{-ikx_n} + \gamma_0(\omega) \delta(t), \quad (12)$$

The inhomogeneous term in (12) provides the jump of the norm of the wavefunction (6)

$$\sum_{n=1}^N |\beta_n(t)|^2 + \int_0^\infty d\omega |\gamma(\omega, t)|^2 + \int_0^\infty d\omega |\delta(\omega, t)|^2, \quad (13)$$

from zero at $t < 0$ to unity at $t > 0$.

We note that as $t \rightarrow \infty$ the qubit amplitude $\beta_n(t) \rightarrow 0$, therefore the norm (13) reduces to:

$$\int_0^\infty d\omega |\gamma(\omega, t \rightarrow \infty)|^2 + \int_0^\infty d\omega |\delta(\omega, t \rightarrow \infty)|^2 = 1. \quad (14)$$

Therefore, the system equations (7), (12), and (9) are now defined for all values of t , negative and positive.

In order to solve the equations (7), (12), and (9) we apply the Fourier transform to the amplitudes $\beta_n(t)$, $\gamma(\omega, t)$, $\delta(\omega, t)$:

$$\beta_n(t) = \int_{-\infty}^\infty \frac{d\nu}{2\pi} \beta_n(\nu) e^{-i(\nu-\Omega)t}, \quad (15)$$

$$\gamma(\omega, t) = \int_{-\infty}^\infty \frac{d\nu}{2\pi} \gamma(\omega, \nu) e^{-i(\nu-\omega)t}, \quad (16)$$

$$\delta(\omega, t) = \int_{-\infty}^\infty \frac{d\nu}{2\pi} \delta(\omega, \nu) e^{-i(\nu-\omega)t}. \quad (17)$$

From (7), (12) and (9) we obtain:

$$\begin{aligned} -i(\nu - \Omega)\beta_n(\nu) &= -i \int_0^\infty d\omega g(\omega) \gamma(\omega, \nu) e^{ikx_n} \\ &- i \int_0^\infty d\omega g(\omega) \delta(\omega, \nu) e^{-ikx_n}, \end{aligned} \quad (18)$$

$$-i(\nu - \omega)\gamma(\omega, \nu) = -ig(\omega) \sum_{n=1}^N \beta_n(\nu) e^{-ikx_n} + \gamma_0(\omega), \quad (19)$$

$$-i(\nu - \omega)\delta(\omega, \nu) = -ig(\omega) \sum_{n=1}^N \beta_n(\nu) e^{ikx_n}. \quad (20)$$

Because both frequency variables ω and ν belong to the continuum we will solve the equations (19) and (20) using the general approach first developed in Heitler's papers and considered in detail in [42], and subsequently used for the study of light scattering by a dense ensemble of atoms [43–45]:

$$\gamma(\omega, \nu) = g(\omega) \sum_{n=1}^N \beta_n(\nu) e^{-ikx_n} \zeta(\nu - \omega) + i\gamma_0(\omega) \zeta(\nu - \omega), \quad (21)$$

$$\delta(\omega, \nu) = g(\omega) \sum_{n=1}^N \beta_n(\nu) e^{ikx_n} \zeta(\nu - \omega), \quad (22)$$

where we introduce a singular zeta function defined as:

$$\zeta(\nu - \omega) = -i\pi\delta(\nu - \omega) + P \frac{1}{\nu - \omega}. \quad (23)$$

In (23), $\delta(\nu - \omega)$ is a Dirac delta-function, and P is a Cauchy principal value.

Next we substitute $\gamma(\omega, \nu)$, $\delta(\omega, \nu)$ in (18) with their expressions (21) and (22). Thus, we obtain a set of linear equations which define the Fourier components of the qubits' amplitudes $\beta_n(\nu)$:

$$\begin{aligned} & \left(\nu - \Omega - 2 \int_0^\infty d\omega g^2(\omega) \zeta(\nu - \omega) \right) \beta_n(\nu) \\ & - 2 \sum_{n' \neq n}^N \beta_{n'}(\nu) \int_0^\infty d\omega g^2(\omega) \cos(k(x_n - x_{n'})) \zeta(\nu - \omega) \\ & = i \int_0^\infty d\omega g(\omega) \gamma_0(\omega) e^{ikx_n} \zeta(\nu - \omega). \end{aligned} \quad (24)$$

Using (23) in (24) we obtain:

$$\begin{aligned} & \left(\nu - \Omega - F(\nu) + i \frac{\Gamma(\nu)}{2} \right) \beta_n(\nu) \\ & + i \frac{\Gamma(\nu)}{2} \sum_{n' \neq n}^N \beta_{n'}(\nu) \left(e^{ik\nu|x_n - x_{n'}|} + iG(k\nu(x_n - x_{n'})) \right) \\ & = i \int_0^\infty d\omega g(\omega) \gamma_0(\omega) e^{ikx_n} \zeta(\nu - \omega), \end{aligned} \quad (25)$$

where (the derivation is given in Appendix A):

$$\begin{aligned} G(k\nu, d_{nn'}) &= -\frac{4}{\Gamma(\nu)} \int_0^\infty d\omega \frac{g^2(\omega) \cos k\nu d_{nn'}}{\omega + \nu} \\ &= \frac{1}{\pi} \cos k\nu d_{nn'} \text{Ci}(|k\nu d_{nn'}|) \\ &+ \frac{1}{\pi} \sin k\nu d_{nn'} \left(-\frac{\pi}{2} \text{sgn}(d_{nn'}) + \text{Si}(k\nu d_{nn'}) \right), \end{aligned} \quad (26)$$

$d_{nn'} = x_n - x_{n'}$, $\Gamma(\nu) = 4\pi g^2(\nu)$, $F(\nu) = 2P \int_0^\infty \frac{g^2(\omega)}{\nu - \omega} d\omega$, $k\nu = \nu/v_g$, $k = \omega/v_g$; $\text{Ci}(x)$ and $\text{Si}(x)$ are the cosine and sine integral functions:

$$\text{Ci}(x) = -\int_x^\infty dt \frac{\cos t}{t}, \quad \text{Si}(x) = \int_0^x dt \frac{\sin t}{t}. \quad (27)$$

Because $\text{Ci}(x)$ is defined for $x > 0$ and $\text{Si}(-x) = -\text{Si}(x)$, the quantity $G(x)$ is the even function, $G(-x) = G(x)$.

It is worthy noting that the equations (25) differ from conventional ones in that they contain the quantity $G(kd_{nn'})$ and Cauchy principal part integral in the right hand side in (25). This modification of the equations for qubits amplitudes appears due to non continuation of the interqubit interaction to negative frequencies.

As the quantity $G(kd_{nn'})$ is a real function it modifies the interaction between qubits giving rise to the shift of their frequencies. In addition, it violates the phase coherence because it is not possible to switch off the interaction between identical qubits simply by taking $kd = n\pi$, where n is integer. We consider the properties of $G(kd)$ in more details in Section V for two-qubit system.

From a set of linear equations (25) we can find N Fourier amplitudes $\beta_n(\nu)$. The next step is to find from (21) and (22) photon Fourier amplitudes $\gamma(\omega, \nu)$ and $\delta(\omega, \nu)$. Finally, from Fourier transform (15), (16) and (17) we find the qubits' and photon amplitudes in a time domain.

However, if we are interested in the scattering amplitudes for $t \rightarrow \infty$ a simpler way is to start from a formal solution of equations (12) and (9):

$$\gamma(\omega, t) = \gamma_0(\omega) - i \sum_{n=1}^N \int_{-\infty}^t d\tau \beta_n(\tau) g(\omega) e^{i(\omega - \Omega)\tau} e^{-ikx_n}, \quad (28)$$

$$\delta(\omega, t) = -i \sum_{n=1}^N \int_{-\infty}^t d\tau \beta_n(\tau) g(\omega) e^{i(\omega - \Omega)\tau} e^{ikx_n}. \quad (29)$$

If we set the upper limit of the integrals (28), (29) to $+\infty$ we obtain:

$$\gamma(\omega, t \rightarrow \infty) = \gamma_0(\omega) - ig(\omega) \sum_{n=1}^N \beta_n(\omega) e^{-ikx_n}, \quad (30)$$

$$\delta(\omega, t \rightarrow \infty) = -ig(\omega) \sum_{n=1}^N \beta_n(\omega) e^{ikx_n}. \quad (31)$$

where $\beta_n(\omega)$ is a solution of equation (25) and is formally given by the inverse Fourier transform of equation (15):

$$\beta_n(\omega) = \int_{-\infty}^{\infty} dt \beta_n(t) e^{i(\omega-\Omega)t}, \quad (32)$$

Below we will show the application of this method to the cases of one and two qubits in a waveguide for which the analytical solutions can be obtained in a closed form.

IV. SINGLE QUBIT

For a single two-level atom located at $x = 0$ the solution of equation (25) is given by:

$$\beta(\omega) = \frac{i \int_0^{\infty} d\omega' g(\omega') \gamma_0(\omega') \zeta(\omega - \omega')}{\left(\omega - \Omega - F(\omega) + i\frac{\Gamma(\omega)}{2}\right)}. \quad (33)$$

With the aid of (30) and (31) we calculate the transmitted and reflected photon amplitudes $\gamma(\omega, t \rightarrow \infty)$ and $\delta(\omega, t \rightarrow \infty)$:

$$\gamma(\omega, t \rightarrow \infty) = \gamma_0(\omega) \frac{\omega - \Omega - F(\omega) + i\frac{\Gamma(\omega)}{4}}{\omega - \Omega - F(\omega) + i\frac{\Gamma(\omega)}{2}} \quad (34)$$

$$+ \frac{g(\omega) P \int_0^{\infty} \frac{d\omega' g(\omega') \gamma_0(\omega')}{\omega - \omega'}}{\omega - \Omega - F(\omega) + i\frac{\Gamma(\omega)}{2}},$$

$$\delta(\omega, t \rightarrow \infty) = \gamma_0(\omega) \frac{-i\frac{\Gamma(\omega)}{4}}{\omega - \Omega - F(\omega) + i\frac{\Gamma(\omega)}{2}} \quad (35)$$

$$+ \frac{g(\omega) P \int_0^{\infty} \frac{d\omega' g(\omega') \gamma_0(\omega')}{\omega - \omega'}}{\omega - \Omega - F(\omega) + i\frac{\Gamma(\omega)}{2}}.$$

As it is seen from $\gamma(\omega, t \rightarrow \infty) - \delta(\omega, t \rightarrow \infty) = \gamma_0(\omega)$, the condition which is only valid for the scattering from a single qubit. The flux conservation is fulfilled not at a single frequency, but as integral quantity (see normalizing condition (14)).

It is worth noting that the second terms in (34) and (35) which contain Cauchy principal value integrals are responsible for the dependence of the scattering spectra on the initial distance between the center of incident Gaussian pulse and the first qubit in the chain.

We note that the derivation of the transmitted and reflected amplitudes (34) and (35) is not restricted to

Wigner-Weisskopf approximation $\Gamma(\Omega) \ll \Omega$. It is also valid for strong coupling where $\Gamma(\Omega) \leq \Omega$.

The evolution of qubit's amplitude $\beta(t)$ is obtained from (15) with $\beta(\omega)$ from (33):

$$\beta(t) = \int_{-\infty}^{\infty} \frac{d\omega}{2\pi} \frac{i \int_0^{\infty} d\omega' g(\omega') \gamma_0(\omega') \zeta(\omega - \omega')}{\omega - \Omega - F(\omega) + i\frac{\Gamma(\omega)}{2}} e^{-i(\omega-\Omega)t}. \quad (36)$$

In Wigner-Weisskopf approximation we can obtain a simple analytical expression for the evolution of qubit's amplitude (36) (see Appendix B):

$$\beta(t) = \int_0^{\infty} d\omega g(\omega) \gamma_0(\omega) \frac{e^{-\frac{\Gamma}{2}t} - e^{-i(\omega-\Omega)t}}{(\omega - \Omega + i\frac{\Gamma}{2})}. \quad (37)$$

The expressions (34), (35) look rather different from the transmitted and reflected amplitudes which were found in a framework of stationary scattering approach for a monochromatic signal scattered by a two-level atom in an 1D open waveguide [48, 49]:

$$\gamma(\omega) = \frac{\omega - \Omega}{\omega - \Omega + i\frac{\Gamma}{2}}, \quad (38)$$

$$\delta(\omega) = \frac{-i\frac{\Gamma}{2}}{(\omega - \Omega + i\frac{\Gamma}{2})}. \quad (39)$$

Here and below Γ is the full width of the spectral lines. Below we show that in some cases the expressions (34) and (35) provide the stationary scattering results.

We assume that the incident wave packet is a narrow pulse which can be approximated by a delta function:

$$\gamma_0(\omega) = A\delta(\omega - \omega_S) = \frac{A}{2\pi} \int_{-\infty}^{+\infty} d\lambda e^{i\lambda(\omega - \omega_S)}. \quad (40)$$

Plugging (40) in (34) and (35) we obtain for principal value integral:

$$\begin{aligned} P \int_0^{\infty} d\omega' \frac{g(\omega') \gamma_0(\omega')}{\omega - \omega'} &\approx g(\omega) \frac{A}{2\pi} \int_{-\infty}^{\infty} d\lambda e^{-i\lambda\omega_S} P \int_{-\infty}^{\infty} d\omega' \frac{e^{i\lambda\omega'}}{\omega - \omega'} \\ &= -i\pi g(\omega) \frac{A}{2\pi} \int_{-\infty}^{\infty} d\lambda e^{-i\lambda\omega_S} e^{i\lambda\omega} = -i\pi g(\omega) A\delta(\omega - \omega_S) \\ &\equiv -i\pi g(\omega) \gamma_0(\omega). \end{aligned} \quad (41)$$

When deriving (41) we first assume that the coupling $g(\omega)$ is a slow function of ω , so that we take it out of the integral. Second, we put the lower bound in principal value integral to minus infinity which allows the

application of Kramers-Kronig relation $P \int_{-\infty}^{+\infty} \frac{e^{i\lambda\omega'}}{\omega-\omega'} d\omega' = -i\pi e^{i\lambda\omega}$.

If we use the result (41) in (34) and (35) and assume that the atom is initially not excited, we obtain for transmitted and reflection amplitudes the expressions which are known from the stationary theories:

$$\gamma(\omega, t \rightarrow \infty) = \gamma_0(\omega) \frac{\omega - \Omega - F(\omega)}{\omega - \Omega - F(\omega) + i\frac{\Gamma(\omega)}{2}}, \quad (42)$$

$$\delta(\omega, t \rightarrow \infty) = \gamma_0(\omega) \frac{-i\frac{\Gamma(\omega)}{2}}{\omega - \Omega - F(\omega) + i\frac{\Gamma(\omega)}{2}}. \quad (43)$$

These expressions are similar to those obtained in the framework of time-dependent approach in [32], where $\gamma_0(\omega)$ was arbitrary pulse shape. However, here the expressions (42) and (43) are valid if the incident photon is a delta pulse (40). For this case, these expressions are exact asymptotic solutions for time dependent scattering of a single-photon pulse from a two-level atom [46].

For arbitrary shape of $\gamma_0(\omega)$ the exact expressions (34) and (35) must be used.

Below we present several plots for qubit's amplitude, forward and backward photon spectra calculated from expressions (37), (34), and (35) for incident travelling Gaussian pulse:

$$\gamma_0(\omega) = \left(\frac{2}{\pi\Delta^2} \right)^{1/4} \exp \left(i(\omega - \omega_s)t_0 - \frac{(\omega - \omega_s)^2}{\Delta^2} \right), \quad (44)$$

where Δ is the width of Gaussian pulse in the frequency domain, $\Delta x = v_g/\Delta$ is the width of Gaussian pulse in space, $t_0 = x_0/v_g$ is the time that it takes for the center of a Gaussian packet to travel from the point $-x_0$ to the point $x = 0$ where the qubit is located. For our parameter values $v_g = 3 \times 10^8$ m/s, $\Omega/2\pi = 5$ GHz, $\Delta/\Omega = 0.1$, the width of the packet in space $\Delta x = v_g/\Delta \approx 10$ cm.

We assume that at the initial time $t = 0$ qubit is in its ground state and the maximum of the envelope of a Gaussian pulse is located at the distance x_0 from the qubit. The plots of qubit's excitation probability $|\beta|^2$ for four values of initial distance x_0 between Gaussian peak and qubit are shown in Fig. 1 for $\Delta/\Omega = 0.1$ and $\gamma = \Gamma/\Omega = 0.05$. Our calculations show that the maximum excitation, $|\beta_{max}|^2 \approx 0.38$, is obtained if x_0 is large compared with the pulse width, v_g/Δ . Similar result ($|\beta_{max}|^2 = 0.4$) was obtained in [31] where the initial position of the peak of the pulse was at the distance $10v_g/\Delta$ from the qubit.

As is known, the maximum excitation $|\beta_{max}|^2 = 0.5$ is achieved when qubit is illuminated from one side by the stationary plane wave [31]. The reason for this is that the qubit-field interaction Hamiltonian allows the transformation of the forward and backward propagating

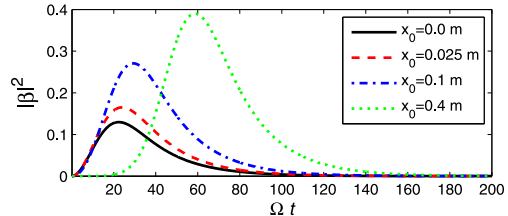


FIG. 1: Probability of the qubit excitation, calculated from (37) for different distances, x_0 of a peak of the incident Gaussian pulse from the qubit. $x_0 = 0$, solid black line; $x_0 = 0.025$ m, dashed red line; $x_0 = 0.1$ m, dashed-dotted blue line; $x_0 = 0.4$, dotted green line. $\Delta/\Omega = 0.1$, $\gamma = \Gamma/\Omega = 0.05$.

continua to a bright B^\dagger and a dark D^\dagger continuum, given by $B^\dagger = (a^\dagger + b^\dagger)/\sqrt{2}$, $D^\dagger = (a^\dagger - b^\dagger)/\sqrt{2}$ [50]. The dark continuum is decoupled from the qubits, allowing 50% of the incident wave $a^\dagger = (B^\dagger + D^\dagger)/\sqrt{2}$ transmit through the waveguide unchanged. The bright component of the incident wave is scattered by the qubits providing 50% of its maximum excitation. The full inversion $|\beta|^2 = 1$ can be obtained with the incident pulse of special shape [51, 52].

We rewrite (34) and (35) in Wigner-Weisskopf approximation, $\Gamma(\omega) = \Gamma(\Omega) \equiv \Gamma$, $g(\omega) = g(\Omega) = (\Gamma/4\pi)^{1/2}$. The frequency shift $F(\omega) = F(\Omega)$ is incorporated implicitly in Ω :

$$\gamma_{WW}(\omega) = \gamma_0(\omega) \frac{\omega - \Omega + i\frac{\Gamma}{4}}{\omega - \Omega + i\frac{\Gamma}{2}} + \frac{\Gamma}{4\pi} P \int_0^\infty \frac{d\omega' \gamma_0(\omega')}{\omega - \omega'}, \quad (45)$$

$$\delta_{WW}(\omega) = \gamma_0(\omega) \frac{-i\frac{\Gamma}{4}}{\omega - \Omega + i\frac{\Gamma}{2}} + \frac{\Gamma}{4\pi} P \int_0^\infty \frac{d\omega' \gamma_0(\omega')}{\omega - \omega'}. \quad (46)$$

We compare these expressions with those obtained in [32] for arbitrary pulse shape and with the extension of the coupling to negative frequencies:

$$\gamma(\omega) = \gamma_0(\omega) \frac{\omega - \Omega}{\omega - \Omega + i\frac{\Gamma}{2}}, \quad (47)$$

$$\delta(\omega) = \gamma_0(\omega) \frac{-i\frac{\Gamma}{2}}{\omega - \Omega + i\frac{\Gamma}{2}}. \quad (48)$$

We note that for Gaussian pulse (44) the approximate probabilities $|\gamma(\omega)|^2$ and $|\delta(\omega)|^2$ do not depend on the initial distance x_0 between Gaussian peak and the qubit.

Below in Fig.2 and Fig.3 we plot the forward, $S_1(\omega) = |\gamma_{WW}(\omega)|^2 \Omega$ and backward, $S_2(\omega) = |\delta_{WW}(\omega)|^2 \Omega$ radiation spectra calculated from exact expressions (45) and

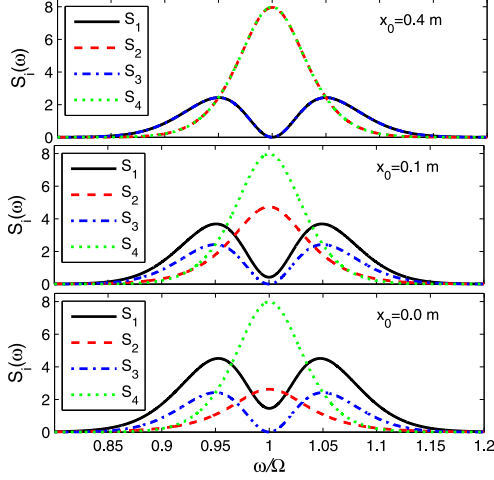


FIG. 2: Photon radiation spectra for scattering of Gaussian pulse (44) by a single qubit for different initial distances of the Gaussian peak from the qubit. $S_1(\omega) = |\gamma_{WW}(\omega)|^2\Omega$ (45), solid (black) line; $S_2(\omega) = |\delta_{WW}(\omega)|^2\Omega$ (46), dashed (red) line; $S_3(\omega) = |\gamma(\omega)|^2\Omega$ (47), dashed-dotted (blue) line; $S_4(\omega) = |\delta(\omega)|^2\Omega$ (48), dotted (green) line. The parameters of the qubit system and initial pulse are as follows: $\omega_s/\Omega = 1$, $\Gamma/\Omega = 0.1$, $\Delta/\Omega = 0.1$.

(46), and systematically compare them with those calculated from (47), $S_3(\omega) = |\gamma(\omega)|^2\Omega$, and (48), $S_4(\omega) = |\delta(\omega)|^2\Omega$.

We study how the photon spectra depend on the distance x_0 of a Gaussian peak from qubit. This behavior is shown in Fig.2 for resonance case, $\omega_s = \Omega$ and in Fig.3 and Fig.4 for small detunings, $\omega_s/\Omega = 1.05$ and $\omega_s/\Omega = 0.95$, respectively. For relative large distance, $x_0 = 0.4 \text{ m} \gg \Delta x$, the exact equations (45) and (46) provide practically the same result as the approximate equations (47) and (48). However, if at the initial instant the Gaussian peak is born closer to the qubit its front wing begins at the same moment to interact with a qubit. Therefore, the spectral lines more and more deviate from large distance results. Finally, we obtain the photon spectra for $x_0 = 0$ as shown in the bottom panel of Fig.2, Fig.3, and Fig.4. We note that in these figures the quantities $S_3(\omega) = |\gamma(\omega)|^2\Omega$ and $S_4(\omega) = |\delta(\omega)|^2\Omega$ calculated from (47) and (48), respectively, do not depend on the distance between the initial position of Gaussian peak and the qubit.

The equations (47) and (48) provide the flux conservation at every frequency: $|\gamma(\omega)|^2 + |\delta(\omega)|^2 = |\gamma_0(\omega)|^2$. However, this simple condition is not valid for exact equations (45) and (46) where the normalization condition has the form of integral quantity (14). For every plot in Fig.2 and Fig.3 we calculated the normalizing quantity $I = \int d\omega |\gamma_{WW}(\omega)|^2 + \int d\omega |\delta_{WW}(\omega)|^2$ where the integration was performed within the frequency span of the plots. In every case, I differs from unity less than a per-

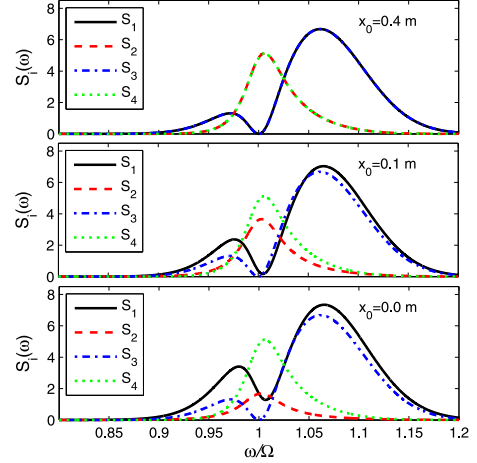


FIG. 3: Photon radiation spectra for scattering of Gaussian pulse (44) by a single qubit, $S_1(\omega) = |\gamma_{WW}(\omega)|^2\Omega$, solid (black) line; $S_2(\omega) = |\delta_{WW}(\omega)|^2\Omega$, dashed (red) line; $S_3(\omega) = |\gamma(\omega)|^2\Omega$, dashed-dotted (blue) line; $S_4(\omega) = |\delta(\omega)|^2\Omega$, dotted (green) line. The parameters of the qubit system and initial pulse are as follows: $\Delta/\Omega = 0.1$, $\Gamma/\Omega = 0.05$, $\omega_s/\Omega = 1.05$.

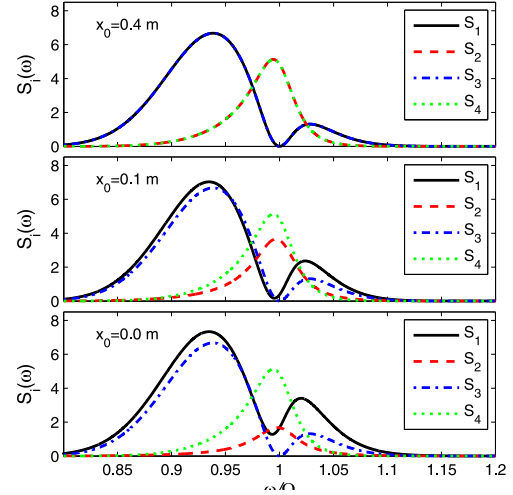


FIG. 4: Photon radiation spectra for scattering of Gaussian pulse (44) by a single qubit, $S_1(\omega) = |\gamma_{WW}(\omega)|^2\Omega$, solid (black) line; $S_2(\omega) = |\delta_{WW}(\omega)|^2\Omega$, dashed (red) line; $S_3(\omega) = |\gamma(\omega)|^2\Omega$, dashed-dotted (blue) line; $S_4(\omega) = |\delta(\omega)|^2\Omega$, dotted (green) line. The parameters of the qubit system and initial pulse are as follows: $\omega_s/\Omega = 1$, $\Gamma/\Omega = 0.05$, $\omega_s/\Omega = 0.95$.

cent.

The major difference between the plots of equations (45), (46) and those of equations (47), (48) is that the transmittance $|\gamma_{WW}(\omega)|^2$ never equals zero at the resonance frequency, $\omega = \Omega$ and the reflectance $|\delta_{WW}(\omega)|^2$ never reaches its maximum value $|\gamma_0(\Omega)|^2$ if the initial distance between Gaussian peak and the qubit is compa-

rable or less than the pulse width. These are the principal part integrals in (45), (46) which are responsible for these properties. From the other hand, the shape of the lines are similar. The transmittance $|\gamma_{WW}(\omega)|^2$ is up shifted relative to $|\gamma(\omega)|^2$, while the reflectance $|\delta_{WW}(\omega)|^2$ is down shifted relative to $|\gamma(\omega)|^2$.

V. TWO-QUBIT SYSTEM

In this section, we study how a single-photon pulse is scattered by a two-atom system coupled to a 1D waveguide. We consider two atoms located at the coordinates $x_1 = 0$ and $x_2 = d$. From equations (25) we obtain two coupled equations for Fourier components of qubits' amplitudes $\beta_1(\nu)$ and $\beta_2(\nu)$:

$$\begin{aligned} & \left(\Delta(\nu) + i\frac{\Gamma(\nu)}{2} \right) \beta_1(\nu) + i\frac{\Gamma(\nu)}{2} \beta_2(\nu) (e^{ik_\nu d} + iG(k_\nu d)) \\ & = C_1(\nu), \end{aligned} \quad (49a)$$

$$\begin{aligned} & \left(\Delta(\nu) + i\frac{\Gamma(\nu)}{2} \right) \beta_2(\nu) + i\frac{\Gamma(\nu)}{2} \beta_1(\nu) (e^{ik_\nu d} + iG(k_\nu d)) \\ & = C_2(\nu), \end{aligned} \quad (49b)$$

where $\Delta(\nu) = \nu - \Omega - F(\nu)$, and:

$$C_1(\nu) = \pi g(\nu)\gamma_0(\nu) + iP \int_0^\infty d\omega \frac{g(\omega)\gamma_0(\omega)}{\nu - \omega}, \quad (50a)$$

$$C_2(\nu) = \pi g(\nu)\gamma_0(\nu)e^{ik_\nu d} + iP \int_0^\infty d\omega \frac{g(\omega)\gamma_0(\omega)e^{ik_\nu d}}{\nu - \omega}. \quad (50b)$$

From (49a) we find the explicit expressions for qubits' amplitudes:

$$\begin{aligned} \beta_1(\nu) &= \frac{\left(\Delta(\nu) + i\frac{\Gamma(\nu)}{2} \right) C_1(\nu)}{\left(\Delta(\nu) + i\frac{\Gamma(\nu)}{2} \right)^2 + \frac{\Gamma^2(\nu)}{4} (e^{ik_\nu d} + iG(k_\nu d))^2} \\ &\quad - \frac{i\frac{\Gamma(\nu)}{2} (e^{ik_\nu d} + iG(k_\nu d)) C_2(\nu)}{\left(\Delta(\nu) + i\frac{\Gamma(\nu)}{2} \right)^2 + \frac{\Gamma^2(\nu)}{4} (e^{ik_\nu d} + iG(k_\nu d))^2}, \end{aligned} \quad (51a)$$

$$\begin{aligned} \beta_2(\nu) &= \frac{\left(\Delta(\nu) + i\frac{\Gamma(\nu)}{2} \right) C_2(\nu)}{\left(\Delta(\nu) + i\frac{\Gamma(\nu)}{2} \right)^2 + \frac{\Gamma^2(\nu)}{4} (e^{ik_\nu d} + iG(k_\nu d))^2} \\ &\quad - \frac{i\frac{\Gamma(\nu)}{2} (e^{ik_\nu d} + iG(k_\nu d)) C_1(\nu)}{\left(\Delta(\nu) + i\frac{\Gamma(\nu)}{2} \right)^2 + \frac{\Gamma^2(\nu)}{4} (e^{ik_\nu d} + iG(k_\nu d))^2}, \end{aligned} \quad (51b)$$

where:

$$G(k_\nu d) = \frac{1}{\pi} \cos k_\nu d Ci(k_\nu d) + \frac{1}{\pi} \sin k_\nu d \left(-\frac{\pi}{2} + Si(k_\nu d) \right). \quad (52)$$

From (30), (31) we obtain the scattering amplitudes for $t \rightarrow \infty$:

$$\begin{aligned} \gamma(\omega, t \rightarrow \infty) &= \gamma_0(\omega) \\ -ig(\omega) &\frac{\left(\Delta(\omega) + \frac{\Gamma}{2} e^{-ikd} G(kd) \right) C_1(\omega)}{\left(\Delta(\omega) + i\frac{\Gamma}{2} \right)^2 + \frac{\Gamma^2}{4} (e^{ikd} + iG(kd))^2} \end{aligned} \quad (53)$$

$$-ig(\omega) \frac{\left(\Delta(\omega) e^{-ikd} + \Gamma \sin kd + \frac{\Gamma}{2} G(kd) \right) C_2(\omega)}{\left(\Delta(\omega) + i\frac{\Gamma}{2} \right)^2 + \frac{\Gamma^2}{4} (e^{ikd} + iG(kd))^2},$$

$$\begin{aligned} i\delta(\omega, t \rightarrow \infty) &= \frac{e^{-ikd}/g(\omega)}{\left(\Delta(\omega) + i\frac{\Gamma}{2} \right)^2 + \frac{\Gamma^2}{4} (e^{ikd} + iG(kd))^2} \\ &= \frac{\left(\Delta(\omega) + \frac{\Gamma}{2} e^{-ikd} G(kd) \right) C_2(\omega)}{\left(\Delta(\omega) + i\frac{\Gamma}{2} \right)^2 + \frac{\Gamma^2}{4} (e^{ikd} + iG(kd))^2} \end{aligned} \quad (54)$$

$$+ \frac{\left(\Delta(\omega) e^{-ikd} + \Gamma \sin kd + \frac{\Gamma}{2} G(kd) \right) C_1(\omega)}{\left(\Delta(\omega) + i\frac{\Gamma}{2} \right)^2 + \frac{\Gamma^2}{4} (e^{ikd} + iG(kd))^2},$$

where $k = \omega/v_g$, $\Gamma \equiv \Gamma(\omega)$, and $C_1(\omega)$, $C_2(\omega)$ are given in (50a), (50b).

We also note here that the derivation of the transmitted and reflected amplitudes (53) and (54) is not restricted to Wigner-Weisskopf approximation $\Gamma(\Omega) \ll \Omega$. It is also valid for strong coupling where $\Gamma(\Omega) \leq \Omega$.

A. The properties of $G(kd)$

From the denominator in (51a),(51b) we find the equations for the resonances (poles) which lie in the lower part of the complex ω plane:

$$\begin{aligned} \Delta_-(\omega) &= -\frac{\Gamma(\omega)}{2} (\sin kd + G(kd)) - i\frac{\Gamma(\omega)}{2} (1 - \cos kd), \\ \Delta_+(\omega) &= \frac{\Gamma(\omega)}{2} (\sin kd + G(kd)) - i\frac{\Gamma(\omega)}{2} (1 + \cos kd), \end{aligned} \quad (55)$$

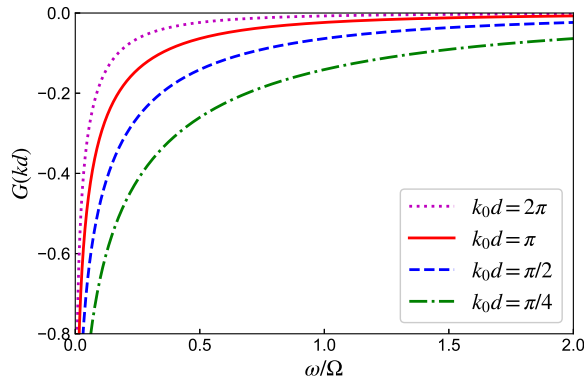


FIG. 5: The frequency dependence of $G(kd)$ for several interqubit distances $d = \lambda, \lambda/2, \lambda/4, \lambda/8$.

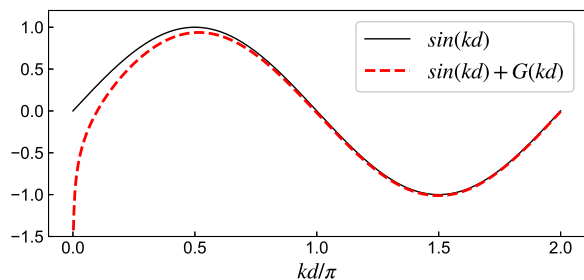


FIG. 6: The difference between $\sin(kd)$ and $\sin(kd) + G(kd)$ vs. kd for frequency $\omega = \Omega$.

where $k = \omega/v_g$. The numerical calculations show that in a vast range of relevant parameters the value $G(kd)$ is rather small (see Fig.5). A noticeable difference between $\sin(kd)$ and $\sin(kd) + G(kd)$ is only observed for $kd < \pi/2$. (see Fig.6). Therefore, for small $k_0d = \Omega d/v_g$ the main contribution to the frequency shift originates from $G(kd)$ (see Fig.7).

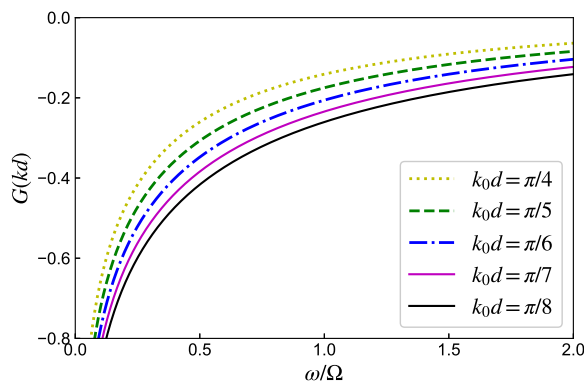


FIG. 7: The frequency dependence of $G(kd)$ in the range $-0.8 < G(kd) < 0$ for several interqubit distances $d = \lambda/8, \lambda/10, \lambda/12, \lambda/14, \lambda/16$.

The number of poles depends on the interqubit distance d . Assuming Wigner-Weisskopf approximation, $\Gamma(\Omega)/\Omega \ll 1$ we may safely replace in the right hand side of equations (55) the running frequency ω with the qubit frequency Ω . Thus, in the plane of complex ω we obtain two poles:

$$\omega_{\pm} = \Omega + \Delta\Omega_{\pm} - i\Gamma_{\pm}, \quad (56)$$

where $\Delta\Omega_{\pm}$ is the frequency shift:

$$\Delta\Omega_{\pm} = F(\Omega) \pm \frac{\Gamma(\Omega)}{2} (\sin k_0d + G(k_0d)), \quad (57)$$

and Γ_{\pm} is the rate of spontaneous emission:

$$\Gamma_{\pm} = \frac{\Gamma(\Omega)}{2} (1 \pm \cos(k_0d)), \quad (58)$$

where $k_0 = \Omega/v_g$.

This two-pole approximation is also called Markovian approximation. It means that we may neglect the retardation effects: two qubits feel the incident photon instantaneously. As was shown in [22] the Markovian approximation is still valid for $k_0d < 5\pi$.

The non-Markovian regime is described by (55) where ω is the running frequency of incident photon. These equations imply that the resonance energies and their widths depend on the frequency of incident photon, which comes in (55) via the the wave vector $k = \omega/v_g$. This is a general feature of non-Markovian behavior when the photon-mediated interaction between qubits is not instantaneous and the retardation effects have to be included. In our method the retardation effects are automatically included since the quantity kd explicitly enters the expressions for the transmission and reflection amplitudes. It is also common to disregard the frequency dependence of spontaneous emission rate Γ keeping it constant. In this case, non-Markovian behavior manifests via the the wave vector $k = \omega/v_g$ [22].

From (57) we see that $G(k_0d)$ is responsible for the frequency shift, therefore, it modifies the interqubit interaction. As is seen from (57) we cannot switch off the interaction between two qubits taking $k_0d = n\pi$, where n is integer. However, for the values k_0d for which $\sin(k_0d) = 0$ this shift is rather small, $\Delta\Omega_{\pm}/\Gamma(\Omega) \ll 1$. On the other hand, for $k_0d \ll 1$, $G(k_0d)$ scales as $1/k_0d$. Therefore, in this case, the contribution from $G(k_0d)$ becomes essential. For example, for $k_0d = 0.01$, $G(0.01) = -1.28$. In this case, $\Delta\Omega_{\pm}/\Gamma(\Omega) = \pm 0.64$. This effect is the evidence of direct dipole-dipole interaction for which low frequency photons are responsible [53].

B. Photon amplitudes

As in the case of a single atom, we can show here that in the frame of Wigner-Weisskopf approximation and for

narrow incident pulse the equations (53) and (54) provide the transmitted and reflected amplitudes which are known from the stationary scattering theories.

The calculation of $C_1(\omega)$ (50a) and $C_2(\omega)$ (50b) for a delta pulse (40) is similar to that of a single atom (41):

$$\begin{aligned} C_1(\omega) &= 2\pi g(\omega)\gamma_0(\omega), \\ C_2(\omega) &= 2\pi g(\omega)\gamma_0(\omega)e^{ik_\omega d}. \end{aligned} \quad (59)$$

Then, assuming the qubits are initially in the ground state and using the equations (30) and (31) we obtain the transmission and reflection spectra for two-qubit system in the Wigner-Weisskopf approximation:

$$\begin{aligned} \gamma(\omega, t \rightarrow \infty) &= \gamma_0(\omega) \frac{\Delta_0^2 - \frac{\Gamma^2}{4} G^2(kd) + i\frac{\Gamma^2}{2} (1 - \cos kd) G(kd)}{(\Delta_0 + i\frac{\Gamma}{2})^2 + \frac{\Gamma^2}{4} (e^{ikd} + iG(kd))^2}, \end{aligned} \quad (60)$$

$$\begin{aligned} \delta(\omega, t \rightarrow \infty) &= -i\frac{\Gamma}{2}\gamma_0(\omega)e^{ikd} \\ &\times \frac{2\Delta_0 \cos kd + \Gamma \sin kd + \Gamma G(kd)}{(\Delta_0 + i\frac{\Gamma}{2})^2 + \frac{\Gamma^2}{4} (e^{ikd} + iG(kd))^2}, \end{aligned} \quad (61)$$

where $\Delta_0 = \omega - \Omega$, $\gamma_0(\omega)$ is the incident delta pulse (40) and $\Gamma \equiv \Gamma(\Omega)$.

Further simplification can be obtained if the distance between qubits is sufficiently large, $kd \gg \pi$. For this

case, within a width of the resonance line the quantity $|G(kd)| \ll 1$ (see Fig.5). Hence, we may disregard $G(kd)$ in the expressions (60) and (61):

$$\gamma(\omega, t \rightarrow \infty) = \gamma_0(\omega) \frac{(\omega - \Omega)^2}{(\omega - \Omega + i\frac{\Gamma}{2})^2 + \frac{\Gamma^2}{4} e^{2ik_\omega d}}, \quad (62)$$

$$\begin{aligned} \delta(\omega, t \rightarrow \infty) &= -i\frac{\Gamma}{2}\gamma_0(\omega)e^{ik_\omega d} \\ &\times \frac{2(\omega - \Omega) \cos(k_\omega d) + \Gamma \sin(k_\omega d)}{(\omega - \Omega + i\frac{\Gamma}{2})^2 + \frac{\Gamma^2}{4} e^{2ik_\omega d}}. \end{aligned} \quad (63)$$

The Markovian approximation is obtained by replacement k_ω with k_Ω in (60), (61), and (62), (63).

The expressions (62), (63) coincide with those obtained in [32] for arbitrary shape $\gamma_0(\omega)$ of the incident pulse and with the extension of the coupling to negative frequencies.

Here we calculate from equations (53) and (54) photon forward, $\gamma(\omega, t \rightarrow \infty)$ and backward, $\delta(\omega, t \rightarrow \infty)$ scattering amplitudes. For simplicity in these equations we assume the rate of spontaneous emission is constant, $\Gamma(\omega) = \Gamma(\Omega) \equiv \Gamma$. However, the non-Markovian non-linear dynamics still exists, since the expressions (53) and (54) depends on photon frequency via $k = \omega/v_g$. Therefore, the expressions (53) and (54) transform as follows:

$$\begin{aligned} \gamma_{WW}(\omega, t \rightarrow \infty) &= \gamma_0(\omega) \\ &\frac{\Gamma}{4} \frac{(\omega - \Omega + \frac{\Gamma}{2} e^{-ikd} G(kd)) \left(i\gamma_0(\omega) + \frac{1}{\pi} P \int_0^\infty d\omega' \frac{\gamma_0(\omega')}{\omega' - \omega} \right)}{(\omega - \Omega + i\frac{\Gamma}{2})^2 + \frac{\Gamma^2}{4} (e^{ikd} + iG(kd))^2} \end{aligned} \quad (64)$$

$$\frac{\Gamma}{4} \frac{((\omega - \Omega) e^{-ikd} + \Gamma \sin kd + \frac{\Gamma}{2} G(kd)) \left(i\gamma_0(\omega) e^{ikd} + \frac{1}{\pi} P \int_0^\infty d\omega' \frac{\gamma_0(\omega') e^{ik'd}}{\omega' - \omega} \right)}{(\omega - \Omega + i\frac{\Gamma}{2})^2 + \frac{\Gamma^2}{4} (e^{ikd} + iG(kd))^2},$$

$$\begin{aligned} \delta_{WW}(\omega, t \rightarrow \infty) &= -e^{ikd} \frac{\Gamma}{4} \frac{(\omega - \Omega + \frac{\Gamma}{2} e^{-ikd} G(kd)) \left(i\gamma_0(\omega) e^{ikd} + \frac{1}{\pi} P \int_0^\infty d\omega' \frac{\gamma_0(\omega') e^{ik'd}}{\omega' - \omega} \right)}{(\omega - \Omega + i\frac{\Gamma}{2})^2 + \frac{\Gamma^2}{4} (e^{ikd} + iG(kd))^2} \\ &- e^{ikd} \frac{\Gamma}{4} \frac{((\omega - \Omega) e^{-ikd} + \Gamma \sin kd + \frac{\Gamma}{2} G(kd)) \left(i\gamma_0(\omega) + \frac{1}{\pi} P \int_0^\infty d\omega' \frac{\gamma_0(\omega')}{\omega' - \omega} \right)}{(\omega - \Omega + i\frac{\Gamma}{2})^2 + \frac{\Gamma^2}{4} (e^{ikd} + iG(kd))^2}. \end{aligned} \quad (65)$$

Below we plot the forward and backward radiation spectra calculated from expressions (64) and (65), and

compare them with those calculated from the expressions (62), (63) obtained in [32].

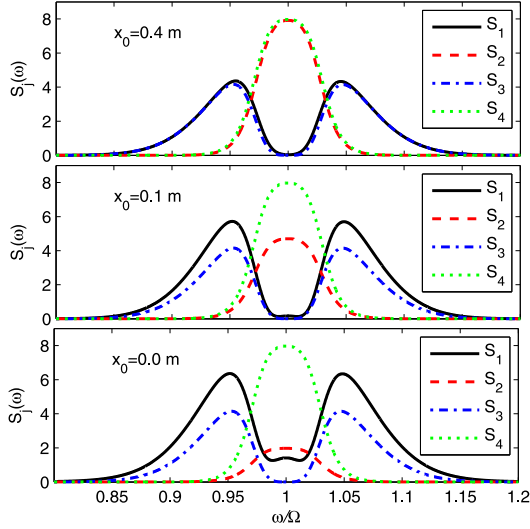


FIG. 8: Photon radiation spectra for different distances of the Gaussian peak from the first qubit for $k_0d = \pi/2$. $S_1(\omega) = |\gamma_{WW}(\omega)|^2\Omega$, solid (black) line; $S_2(\omega) = |\delta_{WW}(\omega)|^2\Omega$, dashed (red) line; $S_3(\omega) = |\gamma(\omega)|^2\Omega$, dashed-dotted (blue) line; $S_4(\omega) = |\delta(\omega)|^2\Omega$, dotted (green) line. The parameters of the qubit system and initial pulse are as follows: $\omega_S/\Omega = 1$, $\Gamma/\Omega = 0.1$, $\Delta/\Omega = 0.1$.

Similar to the one-qubit case, here the photon spectra also depend on the distance x_0 of a Gaussian peak from qubit. This behavior is shown in Fig.8 for $k_0d = \pi/2$ ($d = \lambda/4$). For relative large distance, $x_0 = 0.4$ m $\gg \Delta x$, the exact equations (64) and (65) provide practically the same results as those of approximate equations (62) and (63). As the Gaussian peak becomes closer to the first qubit the spectral lines more and more deviates from large distance results. Finally, we obtain the photon spectra for $x_0 = 0$ as shown in the bottom panel in Fig.8.

As is known, in N-qubit system the Fano interference gives rise to sharp asymmetry of spectral lines [54]. In particular, the reflected amplitude exhibits $N - 1$ zeros which are the manifestation of the Fano interference. For two-qubit system there is a single zero of reflected amplitude on the frequency axis, the position of which depends on qubit parameters, Ω and Γ .

Below we show x_0 - dependence of transmitted and reflected amplitudes for the case of Fano interference.

The transmitted and reflected spectra for $k_0d = 2.25\pi$, and $x_0 = 0.5$ m are shown in Fig. 9. We see that the exact spectra (64),(65) coincide with those calculated from approximate expressions (62), (63). There are two reasons for this. First, the distance between the initial position of Gaussian peak and the first qubit is much larger than the pulse width (50 cm and 10 cm, respectively). Second, the influence of $G(kd)$ on spectral lines for $k_0d = 2.25\pi$ is rather small within the width of line resonances (see Fig.5). A signature of Fano interference

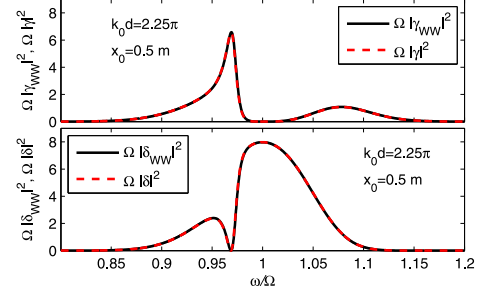


FIG. 9: Photon radiation spectra of a two-qubit system in 1D waveguide for incident Gaussian pulse. The transmitted spectra $|\gamma_{WW}(\omega, t \rightarrow \infty)|^2\Omega$ (solid, black line) and $|\gamma(\omega, t \rightarrow \infty)|^2\Omega$ (dashed, red line) calculated from exact (64) and approximate (62) solutions, respectively, are shown in the upper panel. The reflected spectra $|\delta_{WW}(\omega, t \rightarrow \infty)|^2\Omega$ (solid, black line, and $|\delta(\omega, t \rightarrow \infty)|^2\Omega$ (dashed, red line) calculated from exact (65) and approximate (63) solutions, respectively are shown in the lower panel. The parameters of the qubit system and initial pulse are: $k_0d = 2.25\pi$ and $x_0 = 0.5$ m, $\omega_S/\Omega = 1$, $\Gamma/\Omega = 0.1$, $\Delta/\Omega = 0.1$.

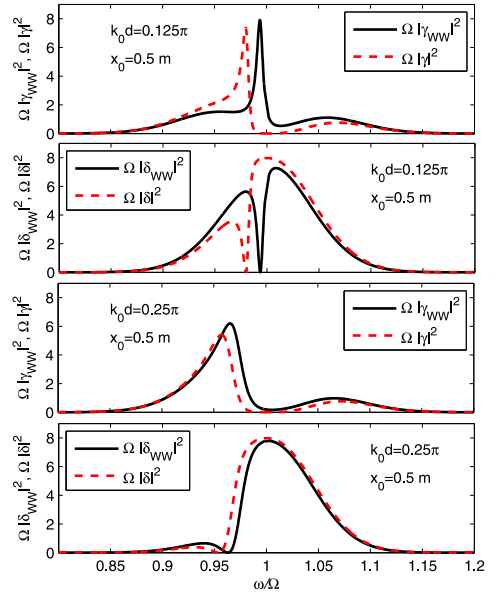


FIG. 10: Photon radiation spectra of a two-qubit system in 1D waveguide for incident Gaussian pulse. The transmitted spectra $|\gamma_{WW}(\omega, t \rightarrow \infty)|^2\Omega$ (solid, black line) and $|\gamma(\omega, t \rightarrow \infty)|^2\Omega$ (dashed, red line) calculated from exact (64) and approximate (62) solutions, respectively, are shown in the upper two panels. The reflected spectra $|\delta_{WW}(\omega, t \rightarrow \infty)|^2\Omega$ (solid, black line, and $|\delta(\omega, t \rightarrow \infty)|^2\Omega$ (dashed, red line) calculated from exact (65) and approximate (63) solutions, respectively are shown in the lower two panels. The parameters of the qubit system and initial pulse are: $x_0 = 0.5$ m, $\omega_S/\Omega = 1$, $\Gamma/\Omega = 0.1$, $\Delta/\Omega = 0.1$.

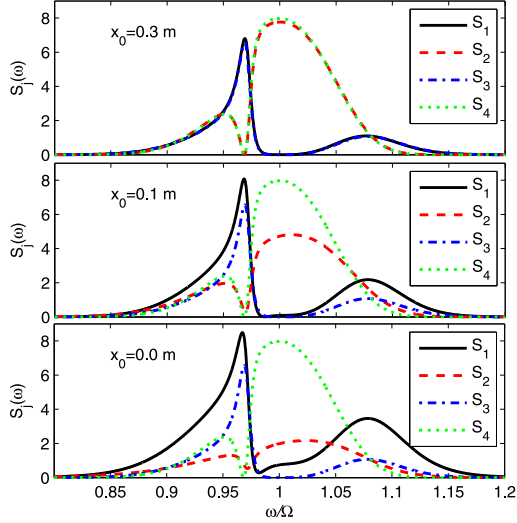


FIG. 11: Photon radiation spectra of a two-qubits for different distance x_0 between the initial position of the pulse peak and the first qubit. All plots show both transmitted ($S_1 = |\gamma_{WW}(\omega, t \rightarrow \infty)|^2 \Omega$, $S_3 = |\gamma(\omega, t \rightarrow \infty)|^2 \Omega$) and reflected ($S_2 = |\delta_{WW}(\omega, t \rightarrow \infty)|^2 \Omega$, $S_4 = |\delta(\omega, t \rightarrow \infty)|^2 \Omega$) radiation spectra. Solid (black) and dashed (red) lines represent the exact solutions (64) and (65), dotted-dashed (blue) and dotted (green) lines represent the approximate solutions (62), (63). The parameters of the qubit system and initial pulse are: $\omega_S/\Omega = 1$, $\Delta/\Omega = 0.1$, $\Gamma/\Omega = 0.1$, $k_0 d = 2.25\pi$.

is seen not only for reflected spectrum (zero in the lower plot in Fig. 9) but also for transmitted spectrum (sharp asymmetrical shape of transmitted line in the upper plot in Fig. 9).

The influence of $G(kd)$ on transmitted and reflected spectra is shown in Fig. 10. Here x_0 is sufficiently large, therefore, the deviation from approximate spectral lines can be attributed to $G(kd)$ in exact expressions. The contribution of $G(kd)$ can be seen by comparison the upper two panels with lower two panels in Fig. 10. The smaller $k_0 d$ the larger $G(kd)$ within the width of the spectral lines. Therefore, for $k_0 d = 0.125\pi$ the deviation of exact resonance lines from approximate ones is larger than that for $k_0 d = 0.25\pi$.

The dependence of transmitted and reflected spectra on the initial distance, x_0 between a Gaussian peak and the first qubit is shown in Fig.11. These plots are calculated for $k_0 d = 2.25\pi$ which makes it possible to neglect the contribution from $G(kd)$ in exact equations (64) and (65) leaving the bare x_0 -dependence. The spectral amplitudes calculated from approximate expressions (62) and (63) do not depend on x_0 . If x_0 is large compared to the pulse width the exact spectral amplitudes are close to the approximate ones (the upper panel in Fig.11). The maximum deviation we see for $x_0 = 0$ (the lower panel in Fig.11).

Finally, we show in Fig.12 the spectral amplitudes for different values, $k_0 d$ calculated for $x_0 = 0$. The radiation

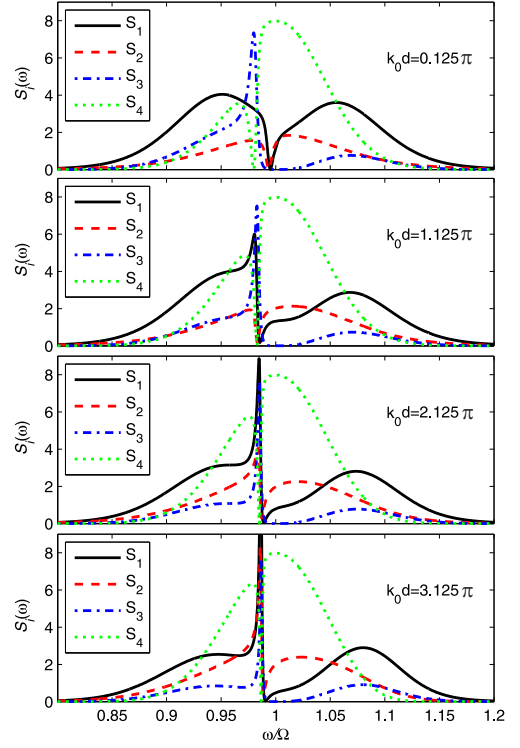


FIG. 12: Photon radiation spectra of a two-qubit system for different values of $k_0 d$. All plots show both transmitted ($S_1 = |\gamma_{WW}(\omega, t \rightarrow \infty)|^2 \Omega$, $S_3 = |\gamma(\omega, t \rightarrow \infty)|^2 \Omega$) and reflected ($S_2 = |\delta_{WW}(\omega, t \rightarrow \infty)|^2 \Omega$, $S_4 = |\delta(\omega, t \rightarrow \infty)|^2 \Omega$) radiation spectra. Solid (black) and dashed (red) lines represent the exact solutions (64) and (65), dotted-dashed (blue) and dotted (green) lines represent the approximate solutions (62), (63). The parameters of the qubit system and initial pulse are: $\Gamma/\Omega = 0.1$, $\Delta/\Omega = 0.1$, $\omega_S = \Omega$, $x_0 = 0$.

spectra are shown in Fig.12 for $k_0 d = 0.125\pi$ ($d = \lambda/16$), $k_0 d = 1.125\pi$ ($d = 9\lambda/16$), $k_0 d = 2.125\pi$ ($d = 17\lambda/16$), $k_0 d = 3.125\pi$ ($d = 25\lambda/16$). The different forms of spectral lines, calculated from exact expressions are only due to the contribution from $G(kd)$. Compare upper panel in Fig.12 where $k_0 d = 0.125\pi$ with the lower panel where $k_0 d = 3.125\pi$.

It also worth noting very sharp and narrow peaks for transmission radiation S_1 . The peak at the bottom panel in Fig.12 ($k_0 d = 3.125\pi$) has its maximum at 14.7 which is not shown in the panel. These narrow peaks are clear signature of the effects of non-Markovianity and sub-radiant transitions, which yields the ultra narrow emission lines.

For every plot in Fig.8-Fig.12 we controlled the normalizing quantity $I = \int d\omega |\gamma_{WW}(\omega)|^2 + \int d\omega |\delta_{WW}(\omega)|^2$ where the integration was performed within the frequency span of the plots. In every case, I differed from unity less than several thousandths.

VI. CONCLUSION

In this paper we analyze the scattering of a single-photon pulse by a one-dimensional chain of two level artificial atoms (qubits) embedded in an open waveguide. The system is described by the continuum mode Jaynes-Cummings Hamiltonian with Hilbert space being truncated to a single excitation subspace. The time-dependent dynamical equations for qubits' amplitudes and for transmitted and reflected photon spectra are solved by application of Heitler's method. Unlike previous approaches our calculations are performed only for physical, positive, frequency axis. This significantly changes the dynamics of the system. First, it leads to the additional photon-mediated dipole-dipole interaction between qubits which results in the violation of the phase coherence between them. Second, the spectral lines of transmitted and reflected spectra crucially depend on the shape of incident pulse. We apply our theory to one-qubit and two-qubit systems. For these two cases we obtain the explicit expressions for the qubits' amplitudes and for the photon spectra. For the travelling incident Gaussian wave packet we calculate the line shapes of transmitted and reflected photons. We show that the transmitted and reflected photon spectra crucially depend on the initial distance of the Gaussian peak from the first qubit. If a distance between the initial position of a pulse peak is comparable to or less than the pulse width in a configuration space the spectral lines are significantly modified. As this distance becomes closer to the qubit, the spectral lines more and more deviate from known results where the continuation of the qubit-photon interaction to the negative frequency axis is used. For two-qubit radiation spectra we thoroughly investigate the influence of $G(kd)$ and position of the pulse peak on Fano interference which gives rise to a sharp asymmetrical form of the the spectral lines.

We believe that the results obtained in the paper may be important for the practical implementation in waveguide QED problems with superconducting qubits where the control and readout pulse generators should be placed as close as possible to the qubit chip at millikelvin temperatures [39].

Our approach can also be further extended and applied to the single-photon scattering by multi-level qubits in strong light-matter coupling regimes.

Acknowledgments

The authors thank O. V. Kibis and A. N. Sultanov for fruitful discussions. The work is supported by the Ministry of Science and Higher Education of Russian Federation under the project FSUN-2023-0006. O. Chuikin acknowledges the financial support from the Foundation for the Advancement of Theoretical Physics and Mathematics "BASIS".

Appendix A: Derivation of equation (26)

We begin with the integral in equation (24):

$$I(\nu) = \int_0^{\infty} d\omega g^2(\omega) \cos(k(x_n - x_{n'})) \zeta(\nu - \omega). \quad (\text{A1})$$

Using (23) we obtain:

$$\begin{aligned} I(\nu) &= -i\pi g^2(\nu) \cos k_\nu d_{nn'} + I_-(\nu) \\ &= -i\pi g^2(\nu) e^{ik_\nu d_{nn'}} + (I_-(\nu) - \pi g^2(\nu) \sin k_\nu d_{nn'}), \end{aligned} \quad (\text{A2})$$

where:

$$I_-(\nu) = -P \int_0^{\infty} d\omega \frac{g^2(\omega) \cos(kd_{nn'})}{\omega - \nu}. \quad (\text{A3})$$

Usually, this integral is calculated by taking $g^2(\omega)$ out of the integral at the frequency ν and moving the lower bound to $-\infty$:

$$I_-(\nu) \approx -g^2(\nu) P \int_{-\infty}^{\infty} d\omega \frac{\cos(\omega t_{nn'})}{\omega - \nu} = \pi g^2(\nu) \sin(\nu t_{nn'}), \quad (\text{A4})$$

where $t_{nn'} = d_{nn'}/v_g$ and we used Kramers-Kronig relation. In this case the second term in brackets in (A2) is zero. Therefore, for $I(\nu)$ we obtain: $I(\nu) = -i\pi g^2(\nu) \exp(i\nu t_{nn'})$.

We would obtain (A4) if we added to $I_-(\nu)$ (A3) the non-RWA counter rotating term $I_+(\nu)$:

$$I_+(\nu) = -P \int_0^{\infty} d\omega \frac{g^2(\omega) \cos(kd_{nn'})}{\omega + \nu}. \quad (\text{A5})$$

If we assume $g^2(\omega) = \lambda\omega$, change variables in the integrand in (A5) ($\omega \rightarrow -\omega$), and add the result to $I_-(\nu)$ we obtain the result which is given in (A4). Strictly speaking, this procedure is not well justified because any frequency dependent coupling ($g^2(\omega)$ in our case) must be exactly zero for negative frequencies.

In order to estimate the contribution from non RWA term more elaborate calculation of $I_-(\nu)$ (A3) is necessary. First, we add and subtract to $I_-(\nu)$ the counter rotating term $I_+(\nu)$: $I_-(\nu) = [I_-(\nu) + I_+(\nu)] - I_+(\nu) = \pi g^2(\nu) \sin(\nu t_{nn'}) - I_+(\nu)$. Therefore, for the second term in right hand side in (A2) we obtain:

$$I_+(\nu) = - (I_-(\nu) - \pi g^2(\nu) \sin k_\nu d_{nn'}). \quad (\text{A6})$$

Next, we begin calculating the quantity $I_+(\nu)$. We

assume $g^2(\omega) = \lambda\omega$. Then, for $I_+(\nu)$ we obtain:

$$\begin{aligned} I_+(\nu) &= -\lambda P \int_0^\infty d\omega \frac{\omega \cos(\omega t_{nn'})}{\omega + \nu} \\ &= -\lambda \int_0^\infty d\omega \cos(\omega t_{nn'}) + \lambda \nu P \int_0^\infty d\omega \frac{\cos(\omega t_{nn'})}{\omega + \nu}. \end{aligned} \quad (\text{A7})$$

To calculate the first term of the right-hand side, we add a small converging factor. This reflects the fact that the system does not respond at high frequencies. In this way, we find that this term vanishes:

$$\begin{aligned} \int_0^\infty d\omega \cos(\omega t_{nn'}) &= \nu \int_0^\infty dy \cos(y \nu t_{nn'}) \\ &= \nu \lim_{\eta \rightarrow 0^+} \int_0^\infty dy e^{-\eta y} \cos y \nu t_{nn'} = \nu \lim_{\eta \rightarrow 0^+} \frac{\eta}{(\nu t_{nn'})^2 + \eta^2} = 0. \end{aligned} \quad (\text{A8})$$

In the integrand of the second term we change variable $x = (\omega + \nu)/\nu$:

$$\begin{aligned} P \int_0^\infty d\omega \frac{\cos(\omega t_{nn'})}{\omega + \nu} &= P \int_1^\infty dx \frac{\cos((x-1)\nu t_{nn'})}{x} \\ &= \cos \nu t_{nn'} P \int_1^\infty dx \frac{\cos(x \nu t_{nn'})}{x} \\ &\quad + \sin \nu t_{nn'} P \int_1^\infty dx \frac{\sin(x \nu t_{nn'})}{x}. \end{aligned} \quad (\text{A9})$$

Two integrals in (A9) can be expressed in terms of sine and cosine integral functions which are given in (27). Therefore, for the quantity $I_+(\nu)$ we obtain:

$$\begin{aligned} I_+(\nu) &= -g^2(\nu) \cos \nu t_{nn'} Ci(\nu |t_{nn'}|) \\ &\quad + g^2(\nu) \sin \nu t_{nn'} \left(\frac{\pi}{2} \operatorname{sgn}(t_{nn'}) - Si(\nu t_{nn'}) \right). \end{aligned} \quad (\text{A10})$$

As is seen from (A10), the quantity $I_+(\nu)$ is the even function of $t_{nn'}$. Therefore we may rewrite (A10) in the following form:

$$\begin{aligned} I_+(\nu) &= -g^2(\nu) \cos \nu t_{nn'} Ci(\nu |t_{nn'}|) \\ &\quad + g^2(\nu) \sin \nu |t_{nn'}| \left(\frac{\pi}{2} - Si(\nu |t_{nn'}|) \right). \end{aligned} \quad (\text{A11})$$

Finally, for $I(\nu)$ we obtain:

$$\begin{aligned} I(\nu) &= -i \frac{\Gamma(\nu)}{4} e^{i\nu |t_{nn'}|} + \frac{\Gamma(\nu)}{4\pi} \cos \nu t_{nn'} Ci(\nu |t_{nn'}|) \\ &\quad + \frac{\Gamma(\nu)}{4\pi} \sin \nu |t_{nn'}| \left(-\frac{\pi}{2} + Si(\nu |t_{nn'}|) \right). \end{aligned} \quad (\text{A12})$$

The insertion of $I(\nu)$ in (24) provides the equation (25) with the quantity $G(kd_{nn'})$ defined in (26).

In fact, according to the derivation the quantity $G(kd_{nn'})$ can be expressed as:

$$G(k_\nu d_{nn'}) = -\frac{4}{\Gamma(\nu)} I_+(\nu) = -\frac{4}{\Gamma(\nu)} \int_0^\infty d\omega \frac{g^2(\omega) \cos k_\nu d_{nn'}}{\omega + \nu}. \quad (\text{A13})$$

Simply speaking, $G(kd_{nn'})$ is the difference between $\pi g^2(\nu) \sin(\nu t_{nn'})$ which accounts for the non RWA contribution ($\pi g^2(\nu) \sin(\nu t_{nn'}) = I_-(\nu) + I_+(\nu)$) and $I_-(\nu)$:

$$G(k_\nu d_{nn'}) = -\frac{4}{\Gamma(\nu)} (\pi g^2(\nu) \sin(\nu t_{nn'}) - I_-(\nu)). \quad (\text{A14})$$

The numerical calculations of $G(kd)$ which are presented in Figs. 5, 7, 6 in the main text show that within resonance width the non-RWA contribution is rather small for $kd_{nn'} > \pi/4$. However, this is not the case if $kd_{nn'} < \pi/4$.

Appendix B: Proof of equation (37)

In the Wigner-Weisskopf approximation $\Gamma(\Omega) \ll \Omega$. Therefore, in (36) we may ignore $F(\omega)$ and replace $\Gamma(\omega)$ with $\Gamma(\Omega) \equiv \Gamma$. Further, we use for $\zeta(\omega - \omega')$ one of its representation:

$$\zeta(\omega - \omega') = \lim_{\sigma \rightarrow 0} \frac{1}{\omega - \omega' + i\sigma}. \quad (\text{B1})$$

Therefore, for (36) we obtain:

$$\begin{aligned} \beta(t) &= i \int_0^\infty d\omega' g(\omega') \gamma_0(\omega') \\ &\quad \times \lim_{\sigma \rightarrow 0} \int_{-\infty}^\infty \frac{d\omega}{2\pi} \frac{e^{-i(\omega - \Omega)t}}{(\omega - \Omega + i\frac{\Gamma}{2})(\omega - \omega' + i\sigma)}. \end{aligned} \quad (\text{B2})$$

There are only two poles in the lower part of the complex ω plane. Applying the Cauchy residue theorem to the second integral in (B2) we obtain the following result:

$$\beta(t) = \int_0^\infty d\omega' g(\omega') \gamma_0(\omega') \frac{e^{-\frac{\Gamma}{2}t} - e^{-i(\omega' - \Omega)t}}{(\omega' - \Omega + i\frac{\Gamma}{2})}, \quad (\text{B3})$$

for $t > 0$ and $\beta(t) = 0$ for $t < 0$.

-
- [1] J. M. Raimond, M. Brune, and S. Haroche, Manipulating quantum entanglement with atoms and photons in a cavity, *Rev. Mod. Phys.* **73**, 565 (2001)., 565 (2001).
- [2] D. Roy, C. M. Wilson, and O. Firstenberg, Strongly interacting photons in one-dimensional continuum *Rev. Mod. Phys.* **89**, 021001 (2017).
- [3] X. Gu, A. F. Kockum, A. Miranowicz, Y.-X. Liu, and F. Nori, Microwave photonics with superconducting quantum circuits, *Phys. Rep.* **718**, 1 (2017).
- [4] A. S. Sheremet, M. I. Petrov, I. V. Iorsh, A. V. Poshakinskiy, and A. N. Poddubny, Waveguide quantum electrodynamics: Collective radiance and photon-photon correlations. *Rev. Mod. Phys.* **95**, 015002 (2023).
- [5] D. Leibfried, R. Blatt, C. Monroe, and D. Wineland, Quantum dynamics of single trapped ions. *Rev. Mod. Phys.* **75**, 281 (2003).
- [6] X. L. Wang, Y. H. Luo, H. L. Huang, M.-C. Chen, Zu-En Su, C. Liu, C. Chen, W. Li, Yu-Q. Fang, X. Jiang, J. Zhang, L. Li, N.-L. Liu, C.-Y. Lu, and J.-W. Pan, 18-qubit entanglement with six photons three degrees of freedom. *Phys. Rev. Lett.* **120**, 260502 (2018).
- [7] X. L. Wang, L. K. Chen, W. Li, H.-L. Huang, C. Liu, C. Chen, Y.-H. Luo, Z.-E. Su, D. Wu, Z.-D. Li, H. Lu, Y. Hu, X. Jiang, C.-Z. Peng, L. Li, N.-L. Liu, Yu-Ao Chen, Chao-Yang Lu, and Jian-Wei Pan, Experimental ten-photon entanglement. *Phys. Rev. Lett.* **117**, 210502 (2016).
- [8] V. Verma, D. Yadav, D. K. Mishra Improvement on cyclic controlled teleportation by using a seven-qubit entangled state. *Optical and Quantum Electronics* **53**, 448 (2021).
- [9] N. Samkharadze, G. Zheng, N. Kalhor, D. Brousse, A. Sammak, U. C. Mendes, A. Blais, G. Scappucci, and L. M. K. Vandersypen, Strong spin-photon coupling in silicon, *Science* **359**, 1123 (2018).
- [10] R. Khordad and H. R. Rastegar Sedehi, Comparison of bound magneto-polaron in circular, elliptical, and triangular quantum dot qubit. *Optical and Quantum Electronics* **52**, 428 (2020).
- [11] P. Krantz, M. Kjaergaard, F. Yan, T. P. Orlando, S. Gustavsson, and W. D. Oliver, A quantum engineer's guide to superconducting qubits. *Appl. Phys. Rev.* **6**, 021318 (2019).
- [12] M. Kjaergaard, M. E. Schwartz, J. Braumüller, P. Krantz, Joel I.-J. Wang, S. Gustavsson, and W. D. Oliver, Superconducting qubits: current state of play. *Ann. Rev. Condensed Matter Phys.* **11**, 369 (2019).
- [13] J. Ruostekoski and J. Javanainen, Arrays of strongly coupled atoms in a one-dimensional waveguide. *Phys. Rev. A* **96**, 033857 (2017).
- [14] K. Lalumière, B. C. Sanders, A. F. van Loo, A. Fedorov, A. Wallraff, and A. Blais, Input-output theory for waveguide QED with an ensemble of inhomogeneous atoms. *Phys. Rev. A* **88**, 043806 (2013).
- [15] D. E. Chang, L. Jiang, A. V. Gorshkov, and H. J. Kimble, Cavity QED with atomic mirrors. *New J. Phys.* **14**, 063003 (2012).
- [16] M. Mirhosseini, E. Kim, X. Zhang, A. Sipahigil, P. B. Dieterle, A. J. Keller, A. Asenjo-Garcia, D. E. Chang, and O. Painter, Cavity quantum electrodynamics with atom-like mirrors. *Nature* **569**, 692 (2019).
- [17] J. D. Brehm, A. N. Poddubny, A. Stehli, T. Wolz, H. Rotzinger, and A. V. Ustinov, Waveguide bandgap engineering with an array of superconducting qubits, *npj Quantum Materials* **6**, 10 (2021).
- [18] A. F. van Loo, A. Fedorov, K. Lalumière, B. C. Sanders, A. Blais, and A. Wallraff Photon-mediated interactions between distant artificial atoms. *Science* **342**, 1494 (2014).
- [19] J.-T. Shen and S. Fan, Theory of single-photon transport in a single-mode waveguide. I. Coupling to a cavity containing a two-level atom. *Phys. Rev. A* **79**, 023837 (2009).
- [20] M.-T. Cheng, J. Xu, and G. S. Agarwal, Waveguide transport mediated by strong coupling with atoms. *Phys. Rev. A* **95**, 053807 (2017).
- [21] Y.-L. L. Fang, H. Zheng, and H. U. Baranger, One-dimensional waveguide coupled to multiple qubits photon-photon correlations. *EPJ Quantum Technol.* **1**, 3 (2014).
- [22] H. Zheng and H. U. Baranger, Persistent Quantum Beats and Long-Distance Entanglement from Waveguide-Mediated Interactions. *Phys. Rev. Lett.* **110**, 113601 (2013).
- [23] D. Roy, Correlated few-photon transport in one-dimensional waveguides: Linear and nonlinear dispersions, *Phys. Rev. A* **83**, 043823 (2011).
- [24] J.-F. Huang, T. Shi, C. P. Sun, and F. Nori, Controlling single-photon transport in waveguides with finite cross section, *Phys. Rev. A* **88**, 013836 (2013).
- [25] G. Diaz-Camacho, D. Porras, and J. J. Garcia-Ripoll, Photon-mediated qubit interactions in one-dimensional discrete and continuous models. *Phys. Rev. A* **91**, 063828 (2015).
- [26] S. Fan, S. E. Kocabas, and J.-T. Shen, Input-output formalism for few-photon transport in one-dimensional nanophotonic waveguides coupled to a qubit, *Phys. Rev. A* **82**, 063821 (2010).
- [27] A. H. Künnerich and K. Molmer, Input-Output Theory with Quantum Pulses. *Phys. Rev. Lett.* **123**, 123604 (2019).
- [28] Ya. S. Greenberg and A. A. Shtygashev, Non hermitian Hamiltonian approach to the microwave transmission through a one-dimensional qubit chain. *Phys. Rev. A* **92**, 063835 (2015).
- [29] Ya. S. Greenberg, A. A. Shtygashev, and A. G. Moiseev, Waveguide band-gap N-qubit array with a tunable transparency resonance. *Phys. Rev. A* **103**, 023508 (2021).
- [30] T. S. Tsoi and C. K. Law, Quantum interference effects of a single photon interacting with an atomic chain. *Phys. Rev. A* **78**, 063832 (2008).
- [31] Y. Chen, M. Wubs, J. Mork, and A. F. Koendrink, Coherent single-photon absorption by single emitters coupled to one-dimensional nanophotonic waveguides, *New J. Phys.* **13**, 103010 (2011).
- [32] Z. Liao, X. Zeng, S.-Y. Zhu, and M. S. Zubairy, Single-photon transport through an atomic chain coupled to a one-dimensional nanophotonic waveguide. *Phys. Rev. A* **92**, 023806 (2015).
- [33] Z. Liao, H. Nha, and M. S. Zubairy, Dynamical theory of single-photon transport in a one-dimensional waveguide coupled to identical and nonidentical emitters. *Phys. Rev. A* **94**, 053842 (2016).

- [34] Z. Liao, X. Zeng, H. Nha, and M. S. Zubairy, Photon transport in a one-dimensional nanophotonic waveguide QED system Phys. Scr. **91**, 063004 (2016).
- [35] C. Zhou, Z. Liao, and M. S. Zubairy, Decay of a single photon in a cavity with atomic mirrors. Phys. Rev. A **105**, 033705 (2022).
- [36] A. Gonzalez-Tudela and D. Porras, Mesoscopic Entanglement Induced by Spontaneous Emission in Solid-State Quantum Optics, Phys. Rev. Lett. **110**, 080502 (2013).
- [37] C. Cohen-Tannoudji, J. Dupont-Roc, and G. Grynberg, Atom-photon interactions. Basic processes and applications. Wiley-VCH GmbH and Co. 2004, p.244.
- [38] Ya. S. Greenberg, A. A. Shtygashev, and A. G. Moiseev, Spontaneous decay of artificial atoms in a three-qubit system. Eur. Phys. J. **B94**, 221 (2021).
- [39] F. Lecocq, F. Quinlan, K. Cicak, J. Aumentado, S. A. Diddams, J. D. Teufel, Control and readout of a superconducting qubit using a photonic link. Nature **591**, 575 (2021).
- [40] K. J. Blow, R. Loudon, and S. J. D. Phoenix, Continuum fields in quantum optics. Phys. Rev. A **42**, 4102 (1990).
- [41] P. Domokos, P. Horak, and H. Ritsch, Quantum description of light-pulse scattering on a single atom in waveguides. Phys. Rev. A **65**, 033832 (2002).
- [42] W. Heitler, The Quantum Theory of Radiation (Oxford University Press, Oxford, 1954).
- [43] I.M.Sokolov, D. V. Kupriyanov, and M.D. Havey, Microscopic Theory of Scattering of Weak Electromagnetic Radiation by a Dense Ensemble of Ultracold Atoms. J. Exp, Theor. Phys. **112**, 246 (2011).
- [44] A. S. Kuraptsev and I. M. Sokolov, Reflection of resonant light from a plane surface of an ensemble of motionless point scatters: Quantum microscopic approach. PRA **91**, 053822 (2015).
- [45] A. S. Kuraptsev and I. M. Sokolov Microscopic Theory of Dipole-Dipole Interaction in Ensembles of Impurity Atoms in a Fabry-Perot Cavity. J. Exp. Theor. Phys. **123**, 237 (2016).
- [46] Ya. S. Greenberg, A. G. Moiseev, and A. A. Shtygashev, Single-photon scattering on a qubit: Space-time structure of the scattered field. Phys. Rev. A **107**, 013519 (2023).
- [47] S. Derouault and M. A. Bouchene, One-photon wave packet interacting with two separated atoms in a one-dimensional waveguide: Influence of virtual photons. Phys. Rev. A **90**, 023828 (2014).
- [48] J.-T. Shen and S. Fan, Coherent photon transport from spontaneous emission in one-dimensional waveguides, Optics Letters **30**, 2001 (2005).
- [49] J. T. Shen and S. Fan, Coherent Single Photon Transport in a One-Dimensional Waveguide Coupled with superconducting Quantum Bits, Phys. Rev. Lett. **95**, 213001 (2005).
- [50] J. T. Shen and S. Fan, Strongly Correlated Two-Photon Transport in a One-Dimensional Waveguide Coupled to a Two-Level System. Phys. Rev. Lett. **98**, 153003 (2007).
- [51] M. Stobinska, G. Alber, and G. Leuchs, Perfect excitation of a matter qubit by a single photon in free space. Europhysics Letters, **86**, 14007 (2009).
- [52] E. Rephaeli, J.-T. Shen, and S. Fan, Full inversion of a two-level atom with a single-photon pulse in one-dimensional geometries. Phys. Rev. A **82**, 033804 (2010).
- [53] S. Derouault and M. A. Bouchene, One-photon wave packet interacting with two separated atoms in a one-dimensional waveguide: Influence of virtual photons. Phys. Rev. A **90**, 023828 (2014).
- [54] D. Mukhopadhyay and G. S. Agarwal, Multiple Fano interferences due to waveguide-mediated phase coupling between atoms. Phys. Rev. A **100**, 013812 (2019).